Submitted to Physical Review

RECEIVED
LAWRENCE
RADIATION LABORATORY

UCRL-20278 Rev.
Preprint

C 2

LIBRARY AND
DOCUMENTS SECTION

COMPARISON OF THE MULTIPERIPHERAL MODEL WITH INCLUSIVE DATA IN K^+p AND π^-p REACTIONS

Jerome H. Friedman and Clifford Risk

October 1971

TWO-WEEK LOAN COPY

This is a Library Circulating Copy which may be borrowed for two weeks. For a personal retention copy, call Tech. Info. Division, Ext. 5545

DISCLAIMER

This document was prepared as an account of work sponsored by the United States Government. While this document is believed to contain correct information, neither the United States Government nor any agency thereof, nor the Regents of the University of California, nor any of their employees, makes any warranty, express or implied, or assumes any legal responsibility for the accuracy, completeness, or usefulness of any information, apparatus, product, or process disclosed, or represents that its use would not infringe privately owned rights. Reference herein to any specific commercial product, process, or service by its trade name, trademark, manufacturer, or otherwise, does not necessarily constitute or imply its endorsement, recommendation, or favoring by the United States Government or any agency thereof, or the Regents of the University of California. The views and opinions of authors expressed herein do not necessarily state or reflect those of the United States Government or any agency thereof or the Regents of the University of California.

COMPARISON OF THE MULTIPERIPHERAL MODEL WITH INCLUSIVE DATA IN K^+p AND π^-p REACTIONS

Jerome H. Friedman

Lawrence Berkeley Laboratory
University of California
Berkeley, California 94720

and

Clifford Risk

Lawrence Berkeley Laboratory
University of California
Berkeley, California 94720

and

Department of Physics
University of California
Davis, California 95616

October 28, 1971

ABSTRACT

The predictions of the multiperipheral model are compared to inclusive data in K^+p and π^-p reactions. We compare with topological longitudinal momentum distributions, double differential distributions, multiplicity cross-sections, π^+/π^- ratio, asymmetry characteristics, isotropy in the cm, and Regge behavior near the kinematical limit. The agreement is reasonably good. We discuss the relation of this work to earlier work on the multi-Regge model, to results of other models, and to the results obtained by other types of approaches to the inclusive analysis.

I. INTRODUCTION

During the last two years the inclusive[1, 2] type of reaction $a + b \rightarrow c +$ anything has become a popular means of studying high energy collisions. Two different approaches to this study can perhaps be distinguished.

On the one hand, detailed studies have been made of the momentum distribution of particle " c " in the momentum regions near the kinematical limit. For example, comparisons of a given reaction (e.g. $\pi^- + p \rightarrow \pi^- +$ anything for slow π^- in the lab.[3]) at several energies have been made to test the Yang conjecture[2] of limiting distributions. Comparisons of the π^- distribution of proton targets with different incident particles have been made[4] to test the factorization hypothesis[5]. Finally, studies of a single reaction at a single energy have been made to test the quantitative predictions of the Regge limit near the kinematical boundary[6]. The advantage of this type of approach is that by examining this momentum range in such detail with these various methods, one can perhaps obtain insight into the precise character of the production process. However, the scope of the knowledge is limited — for example, little is said about the distribution at $p_L \sim 0$, or about its dependence on prong number, or about correlations between the spectra of different types of secondaries (for example, in a p p reaction the relation between fast produced π^- spectra and inelastic p spectra).

On the other hand, various dynamical models have been proposed that describe the spectra over the entire momentum range. For example, we list: (a) the multiperipheral model in the exclusive form of ABFST[7], Chew and Pignotti[8], and CLA[9]; and in the inclusive form of Caneschi and Pignotti[10]; (b) the thermodynamical model

of Hagedorn[11], and (c) the two-fireball model[12,13]. These models have been then compared to a large amount of experimental data. The advantage of this type of approach is that one has a dynamical scheme to potentially describe all aspects of the data. However, in describing the data phenomenologically, there are often free parameters to adjust. Therefore, one must carefully express those features of the predictions that are generally unique to the model and those features that arise from adjusting the free parameters, and then propose tests distinguishing between different models that describe the same data equally well.

In this paper we present a fairly detailed comparison of a particular model - the multi-Regge model - with inclusive data in K^+p and π^-p reactions. In section II, we discuss the model formulated for this comparison. In section III, we present the results of the comparison. Where appropriate, we make reference to the model's description of the inclusive behavior in the Regge limit near the kinematical boundaries. In section IV, we compare our own work to earlier work on the multi-Regge model, propose further areas of development of the model, and compare the multi-Regge model to other kinds of production models.

II. THE MULTI-REGGE MODEL

The multi-Regge model we use is described by the diagrams of Fig. 1. Fig 1a describes the process in which the incident proton and meson emerge peripherally, with the produced secondaries emitted internally from the multi-Regge chain. In a high energy collision, the incident particles can also form resonances that decay backwards, giving rise to fast produced secondaries and large inelasticity of the incident particles. These processes are taken into

account by the diagrams of Fig. 1b-1d. In Fig. 1b, the incident proton emits a π^- and propagates as a Δ^{++} Reggeon, emerging as the second particle in the chain; this process is dualistically equivalent to the backward decay of N* resonances formed by the incident proton. In Fig. 1c, the incident K^+ emits a π^-, and propagates as an exotic m^{*++} meson; this represents the backward decay of K* resonances. Similarly, in Fig. 1d the incident π^- emitting a π^+ and propagating as an m^{*--} resonance, corresponds to backward decay of resonances in the $\pi^+\pi^-$ system.

The amplitude for any of these diagrams is given by

$$A_n(s,t) = (g^2)^{n-2} \prod_{i=1}^{n-1} \left(\frac{b+s_i}{s_i}\right)^{\alpha_i(t_i)} \beta_i(t_i), \qquad (1)$$

and the cross section is given by

$$\sigma_n = \frac{c}{p_0} \int |A_n(s,t)|^2 \, d^n\Phi \qquad (2)$$

Here, s_i and t_i are the invariant subenergies squared and momentum transfers squared of the individual links of the chain; α_i and β_i are the trajectory and residue of the corresponding exchanged Reggeon; b is a constant introduced in order for the s_i dependence to reduce to phase space for small energies; g^2 is the internal m m π coupling constant; and c is a constant giving the normalizations for the separate processes of Figs. 1a-1d. In Eq. (2) $d^n\Phi$ is the volume element for n - body phase space; p_0 is the incident momentum.

In this paper we have used two trajectories - an effective meson trajectory α_m corresponding to the internal Reggeon "m" of Fig. 1, and a baryon trajectory α_B corresponding to the Reggeon Δ^{++} of Fig. 1b. To keep the model as simple as possible, we have used for the Reggeon m* the same parameters as for the Reggeon m.

The parameters for the Reggeons "m" and "B" were determined in an earlier comparison[14] of p p counter data with an inclusive multi-Regge model, and so are fixed in advance; values of α_m, α_B, β_m, and β_B are given in Ref. 14. The constant "b" in Eq. (1) was taken in all cases to be 1 GeV^2. We now have four parameters - the coupling constant g^2 and the normalization of the three processes of Figs. 1a, 1b, and 1c (or Fig. 1d for the $\pi^- p$ reaction).

To evaluate the predictions of the model, we sum incoherently all diagrams for the three processes of Fig. 1 with multiplicities ranging from 2 to 14. The numerical integrations of Eq. (2) over n-body phase space are done with the LBL Monte Carlo program SAGE[15], giving an event-by-event generation of interractions. For each event, charges are assigned by sampling from the Chew-Pignotti alternating I-spin algorithm.[8] We then compare the distributions of these charged particles with the experimental data.

III. PREDICTIONS OF THE MODEL

The data we compare with consist of:

$$K^+ + p \rightarrow \pi^- + \text{anything} \qquad (12\ GeV/c) \qquad (1)$$

$$\pi^- + p \rightarrow \pi^\pm + \text{anything} \qquad (25\ GeV/c) \qquad (2)$$

Reaction (1) has been reported by Ko and Lander[16] and reaction (2) by Elbert, Erwin, and Walker.[17]

Reaction (1)

We will discuss first the model description of the data from reaction (1). The data are shown in Fig. 2. They consist of the inclusive distribution $d\sigma/dp_L$ for given topologies and over all events (Fig. 2a) and the double distribution $Ed^3\sigma/d^3p$ (Fig. 2b). To describe these data with the model, we normalized (see Fig. 2c) the process of Fig. 1a to the distribution at $p_L \sim 0$, Fig. 1b to $p_L > 1.0$ GeV/c, and

Fig. 1c to $p_L < -1.0$ GeV/c. The entire distributions of Figs. 2a, 2b are now predicted over the entire range of both p_L and p_T. Moreover, once the coupling constant g^2 is picked, the normalizations and shapes of the topological p_L- distributions in Fig. 2a are predicted by the model with no free parameters. Finally, with our model fixed by the π^- distributions, the π^+ distribution is predicted in advance. We compare this prediction with the data of reaction (2) below. We now discuss the main characteristics of the data and their interpretation in the model.

1. $d\sigma/dp_L$ Distribution

The data of Figs. 2a, 1b both show pions produced predominantly at $p_L \sim 0$. The multiperipheral model accounts for this by having most pions produced in the internal portion of the diagrams of Fig. 1.[18] For large beam momenta, $p_0 > 100$ GeV/c, it has been shown[19] that the momentum spectra of pions produced in Fig. 1a takes the scaling form

$$\int \frac{E\, d^2\sigma}{dp_T^{\,2}\, dp_L}\, dp_T^{\,2} = F(x) \qquad (3a)$$

At present accelerator energies, the structure function F depends on p_L, being flat over an interval $|x| < L$ that becomes progressively smaller at increasing momenta. For $p_0 > 100$ GeV/c, F is flat for $|x| \leq 0.6$.[19]

2. Asymmetry

Both Fig. 2a, 2b show an asymmetry in the π^- distribution, with the π^- produced preferentially for $x > 0$. This asymmetry was first observed in reaction (2) by Elbert, Erwin and Walker,[17] who reported that the p_L distribution became asymmetric in the Lorentz frame in which the ratio of incident π^- momentum to proton momentum

is 2/3. Since this frame would be the c.m. system for quark-quark interactions in the triplet quark model, this result was presented as evidence for a quark model of meson-baryon collisions. However, they pointed out that this result was obscured by the variation of the asymmetry with the topology of the reaction, being most pronounced for the four-prong interaction and diminishing with increasing prong number, and by the experimental difficulty of separating the leading π^- secondary from the produced secondaries.

The K^+p reaction is free from the problem of leading particle contamination in the distribution of produced secondaries.[20] An asymmetry is again observed, being most pronounced at low multiplicity (Fig. 2a), and again vanishing in the system in which the incident K^+ momentum is 2/3 that of the target proton.

In the multiperipheral model, this asymmetry can be easily understood, coming from two effects:

a) First, there is the obvious effect of the differing proton and K^+ masses.[21] The proton, being relatively heavy, can emit the exchanged Reggeon of Fig. 1a and still continue with large elasticity. The K^+, on the other hand, being lighter, emerges with a smaller momentum in the c.m. Conservation of the produced secondaries to emerge preferentially with $x > 0$ in the c.m. This effect can be seen in Fig. 2c, where we show the p_L distribution of π^- from Fig. 1a alone; these pions account for most of the distributions with $|x| < .5$. In Fig. 2d, we show the predictions for the p_L-distribution for the nucleon and kaon that come from Fig. 1a. The higher elasticity of the nucleon relative to the kaon can be easily seen.[22]

b) In the momentum range with $|x| > .5$, the asymmetry is due to the difference between backward π^-p elastic scattering on the one hand,

with backward π^-K^+ elastic scattering on the other. In this momentum range, the π^- spectra comes from π^- produced peripherally in Figs. 1b, 1c. The relative probabilities of these processes in Fig. 1b, 1c are in turn related to the relative rates for the backward elastic π^-p process at the proton end of the chain in Fig. 1b and the backward π^-K^+ process at the K^+ end of Fig. 1c. However, π^-p two body scattering is relatively much more peripheral than π^-K^+ scattering, since the π^-K^+ process is resonance-dominated to much higher c.m. momenta.[23] Consequently, the π^- spectra for $x < -.5$ is depleted relative to the π^- spectra for $x > .5$.

3. Prong Distribution

In the multiperipheral model, the single constant g^2 determines the relative magnitudes of the multiplicity cross-sections σ_n. The topological cross sections are then fixed through the Chew-Pignotti charge algorithms. In Fig. 2a we see that both the magnitudes and shapes of the topological p_L- distributions are adequately described by the model. In particular, note that the model accounts for the decrease of the asymmetry with the increasing prong number. In the multiperipheral model, this arises from the increasing number of centrally produced π^- together with the restrictions of phase space at larger multiplicity; these two factors serve to reduce the influence of the end effects that led to the asymmetry.

The model predictions for the multiplicity cross sections are shown in Fig. 2e. Curve (a) shows the cross-sections σ_n for n particles in the final state predicted by Fig. 1a. Curve (b) shows the topological cross sections predicted after charge assignments. Curve (c) shows the topological cross sections predicted after Figs. 1b, 1c are included. They are in reasonable agreement (to within 20%) with preliminary experimental data.[24]

4. Double Distributions

The differential cross section of Fig. 2b is adequately described by the model over the entire p_L, p_T range. As pointed out by Ko and Lander, the distribution does not factorize into separate functions of p_L and p_T alone. At $x \sim 0$ and $x \sim 1$, the p_T distribution is much more peaked than at $x \sim .5$.[25] In the multiperipheral model this arises in the following way:[14] Pions at $|x| \sim 1$ are produced peripherally by the mechanisms of Figs. 1b, 1c and hence emerge forward and at small angles. Their distributions can be described in the Regge limit[26] by

$$d^3\sigma = \frac{d^3p}{E} (1 - x)^{1 - 2\alpha(t)} \beta^2(t) \qquad (4)$$

Pions produced internally (but not at $x \sim 0$) are allowed to emerge at larger p_T than the "singly scattered" pions produced at $|x| \sim 1$. At $x \sim 0$, the average p_T again becomes small, a phase space effect.[27]

5. Isotropy and Non-Scaling Behavior

Erwin, Ko, Lander, Pellett, and Yager[28] have recently shown that the spectrum for π^- with small p_L in the c.m. is consistent with isotropy. They plot the distribution at fixed E π^- as a function of $\cos\theta_{\pi^- K^+}$ (see Fig. 2f). For small E, no dependence on $\cos\theta$ is observed, and hence the momentum spectrum takes the form

$$d^3\sigma = \frac{d^3p}{E} f(E). \qquad (3b)$$

This distribution is clearly inconsistent with (3a).

This result is not unexpected. It can be interpreted as an effect of phase space. At small p_L, the distribution (see Fig. 1a) is dominated by high multiplicity events. For example, the low multiplicity 4 prong, 4C final state accounts for only 20% of the 4 prong cross section. Moreover, π^- from these events can kinematically contribute to large $|x|$ values; consequently, their contribution at small $|x|$ is relatively

even smaller. If we now take into account peripherality of the incident K^+ and p, and hence the relatively large energy they emerge with, and subtract this energy and the energy of the rest masses of the produced secondaries from the low c.m. energy (5GeV), we infer that π^- at $p_L \sim 0$ are associated with higher multiplicity events in which most of the other produced secondaries are also at small p_L. Phase space plays a dominant role in these processes, and the phase space integrals alone give an isotropic distribution.

In Fig. 2f, the solid lines give the prediction of the process of Fig. 1a alone, which dominates the distribution at small p_L. The good agreement comes from the model building in the high elasticity of the incident particles and the correct evaluation of the phase space integrals.

Reaction (2)

Next we discuss the data of reaction (2). In Fig. 3a the distribution is shown for forward π^+ and backward π^-, and in Fig. 3b the π^- distribution overall

To compare the model with these data, we evaluated the processes of Figs. 1a, b, c, keeping the same relative normalizations for the three processes as used for Fig. 1a, b, c in the comparison with the K^+p data. Thus, there is only one free parameter — the normalization of the sum.[29] The new features we discuss in our comparison are the following:

1. Ratio of π^+ to π^-

The ratio of the π^+ rate to the π^- rate at $x = 0$ (Fig. 3a) is fixed in the model by the incident charges and the charge-tagging algorithm, and adequately describes the data. In addition, the shapes of each are accounted for. The π^- rate for $p_L > 0$ is enhanced and the π^- rate for $p_L < 0$ is depressed by the asymmetry effects discussed earlier.

2. p_L distribution for π^-

In Fig. 3b we compare the theory with the data for the π^- distribution over all p_L. The agreement is good over the entire p_L range except for $p_L \sim 3$ GeV/c. Here, diffractively produced quasi-two body processes can contribute to the spectrum (e.g. $\pi^- + p \rightarrow \pi^- + N^*$), and these have not been incorporated into our multiperipheral model. Note that for $x < 0$, our prediction is expected to be good because this portion of the spectrum is relatively independent of the identity of the beam particle. Hence, the good agreement with the K^+p data for $x < 0$ leads to good agreement here, too.

IV. SUMMARY

The present work, and its rather good agreement with the data, is not viewed as a positive proof of multi-peripheralism, but rather as a further step in the development of this idea and its comparison with data. This type of phenomenological comparison was quantitatively developed first in the work of CLA (Ref. 9 and earlier work cited there). However, in that work and subsequent work, only specific reactions with a fixed number of identifiable particles in the final state were considered. In the Chew and Pignotti model, a comprehensive attempt is made to predict the relative rates of the multiplicity cross sections and to construct the total cross section from the inelastic multiperipheral processes. In particular, the contributions of Pomeron exchanges is regarded as small. Comparisons of this model to data were subsequently performed, but they have often made approximations in evaluating the phase space integral of Eq. (2), or else evaded this problem by discussing the model in an integral equation framework. The model seems to have been first quantitatively compared to inclusive data with the phase space integrals

performed correctly in the analysis of the Michigan-Wisconsin data (Ref. 19). The present work represents an improvement over the methods used in Ref. 19, and a more careful comparison with detailed data.

Obviously, still further improvements can be made in the model. Inclusion of nucleon resonances, possible inclusion of internally produced resonances, and incorporation of diffractive processes can be added as further comparisons are made. Evaluation of the full ABFST model, in which the freedom in parameters is greatly reduced, should be pursued. Most important, tests should be formulated which can distinguish between the multiperipheral model and other models that could also agree with the inclusive type of data compared herein. In particular, the diffractive model of Hwa[30] and the thermodynamic model of Hagedorn have both had success in describing some aspects of the K^+p data, although the underlying physics of all three models are very different. The present comparison has tested only the following features of multiperipheralism: peripherality of incident particles, p_T cut-off of secondaries, correct treatment of phase space integrals, and correct prediction of topological cross-sections. Some of these features can be incorporated in the other two models, and what is needed are tests to distinguish between the three models. Work is in progress in this area and will be reported presently.

ACKNOWLEDGMENTS

We thank W. Ko and R. Lander for many stimulating discussions during the course of the work. We also acknowledge helpful discussions with R. Hwa, G. Lynch, and D. Lyon.

Work done under the auspices of the U. S. Atomic Energy Commission.

REFERENCES

1. R. P. Feynman, in Proceedings of the Third International Conference on High Energy Collisions, Stony Brook, 1969, edited by C. N. Yang et al. (Gordon and Breach, New York, 1969).

2. J. Benecke, T. T. Chou, C.N. Yang, and E. Yen, Rev. 188, 2159 (1969).

3. W. D. Shephard, J. T. Powers, N. N. Biswas, N. M. Cason, V. P. Kenney, R. R. Riley, D. W. Thomas, J. W. Elbert, and A. R. Erwin, Notre-Dame-Wisconsin preprint, August, 1971.

4. M.-S Chen, R. R. Kinsey, T. W. Morris, R. S. Panvini, L.-L Wang, T. F. Wong, S. L. Stone, T. Ferbel, P. Slattery, B. Werner, J. W. Elbert, and A. R. Erwin, Phys. Rev. Lett. 26, 1585 (1971).

5. A. H. Mueller, Phys. Rev. D2, 2963 (1970); C.E. De Tar, C.E.Jones, F. E. Low, J. H. Weis, J. E. Young, and C.-I. Tan, Phys. Rev. Lett. 26, 672 (1971).

6. R. D. Peccei and A. Pignotti, Phys. Rev. Lett. 26, 1076 (1971); C. Risk, UCRL-20841, June, 1971 (submitted to Phys. Rev.).

7. D. Amati, S. Fubini, and M. Tonin, Nuovo Cimento 25, 626 (1962).

8. G. F. Chew and A. Pignotti, Phys. Rev. 188, 2508 (1969).

9. C.-H. Mo, J. Loskiewicz, and W. W. M. Allison, Nuovo Cimento 57, 93 (1968).

10. L. Caneschi and A. Pignotti, Phys. Rev. Lett. 22, 1219 (1969).

11. R. Hagedorn, Nucl. Phys. B24, 93 (1970).

12. R. K. Adair, Phys. Rev. 172, 1370 (1968).

13. R. C. Hwa, Phys. Rev. Lett. 26, 1143 (1971).

14. C. Risk and J. H. Friedman, Phys. Rev. Lett. 27, 353 (1971).

15. J. H. Friedman, G. R. Lynch, C. Risk, and T. A. Zang, J. Comp. Phys. 8, 144 (1971).

16. W. Ko and R. L. Lander, Phys. Rev. Lett. 26, 1064, 1284 (1971).

17. J. W. Elbert, A. R. Erwin, and W. D. Walker, Phys. Rev.

18. L. Caneschi, D. E. Lyon, Jr., and C. Risk, Phys. Rev. Lett. 25, 774 (1971).

19. D. E. Lyon, Jr., A. E. Bussian, G. D. De Meester, L. W. Jones, B. W. Loo, P. V. Ramana Murthy, R. F. Roth, F. E. Mills, J. G. Learned, D. D. Reeder, B. Cork, and C. Risk, Phys. Rev. Lett. 26, 728 (1971).

20. Similar remarks can be made about the reaction $\pi^+ + p \rightarrow \pi^- +$ anything, N. N. Biswas, N. M. Cason, M. S. Farber, V. P. Kenney, J. D. Poitier, J. T. Powers, O. R. Sander, and W. D. Shephard, Phys. Rev. Lett. 26, 1589 (1971).

21. This mass effect was first discussed for the $\pi^- p$ reaction by L. Caneschi, Phys. Rev. 3D, 2865 (1971), who used a form of the Caneschi and Pignotti model (Ref. 10) to evaluate the inclusive distribution and prong asymmetries utilizing three-body phase space. The present report represents a comprehensive investigation of the predictions of the full multi-Regge model. See also J. H. Friedman and C. Risk, UCRL-20278, February 1971 (unpublished). An explanation for the asymmetry had been given earlier by C. N. Yang, in Proceedings of the Third International Conference on High Energy Collisions, Stony Brook, 1969, ed. by C. N. Yang et al. (Gordon and Breach, New York, 1969).

22. For the two-body process $K^+p \rightarrow K^+p$, conservation of momentum forces both secondaries to emerge symmetrically that this symmetry does not occur in the production process can be seen, for example, in the exclusive reaction $K^-P \rightarrow K^-p\,\pi^+\pi^-$, Fig. 2 of O. Czyzewski, Proceedings of the 14th International Conference on High Energy Physics,

Vienna 1968, edited by J. Prentki, and J. Steinberger (CERN, Geneva, 1968).

23. We have represented this resonance-dominated amplitude with the effective meson "m" of Fig. 1. Other analysis suggest that the intercept $\alpha(0)$ of the exotic meson m* is lower, with $\alpha(0) \sim -.8$. This would give a faster fall-off with energy in the $\pi^- K^+$ backward process, but would still be relatively less peripheral than the $\pi^- p$ process, which is characterized by a trajectory with intercept $\alpha_B(0) \sim -2.0$. For the α_B analysis see Ref. 6, and for the exotic meson analysis see W. Ko, R. Lander, and C. Risk, Phys. Rev. Letters (to be published).

24. M. A. Garnjost (private communication).

25. This dependence of the p_L- distribution on the p_T- value has been discussed, for example, in Ref. 9, Fig. 21.

26. For a discussion of Eq. (4), see Ref. 6 Eq. (4) also expresses the asymmetry effect. For $x \sim -1$, the low intercept of the effective Δ^{++} trajectory, namely $\alpha(0) \sim -2$, leads to a rapid attenuation in the π^- distribution. For $x \sim +1$, the relatively higher intercept of the exotic K^{*++} meson leads to a relatively larger π^- rate.

27. This phase space effect can be seen by evaluating the n-body phase space integrals exactly for massless secondaries. Details will be presented elsewhere. See also the discussion of Ref. 9.

28. J. Erwin, W. Ko, R. L. Lander, D. E. Pellett, and P. M. Yager, Davis preprint, September, 1971.

29. In the approach of Ref. 1-5, the asymptotic ratio of the $\pi^- p$ distribution to the K^+p distribution is predicted to be the ratio of their asymptotic cross sections.

30. R. C. Hwa, Phys. Rev. Letters (to be published).

FIGURE CAPTIONS

Fig. 1. Multi-Regge diagrams: M-projectile meson; p-target proton; m, m*-exchanged mesons; Δ^{++} - exchanged baryon.

Fig. 2. The inclusive data of the K^+p reaction.

(a) longitudinal momentum distribution for various final state topologies.

(b) double differential distribution.

(c) contributions of the separate processes of Fig. 1a; long dashes-Fig. 1a, short dashes-Fig. 1b, dot-dashes-Fig. 1c.

(d) p_L- distributions for the K^+ and p of Fig. 1a.

(e) multiplicity cross sections predicted by the model (see text).

(f) double differential distribution at fixed E plotted against $\cos\theta$ (see text); histogram-data; curve-theory.

Fig. 3. The inclusive data of the π^-p reaction.

(a) π^- backward and π^+ forward.

(b) π^- over the entire p_L range.

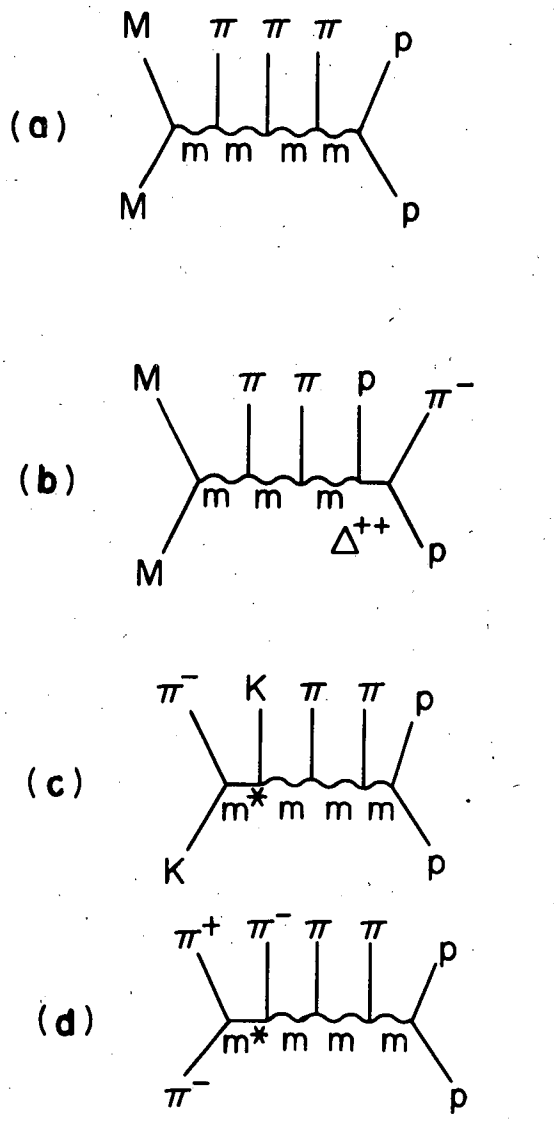

XBL7111-4768

Fig. 1

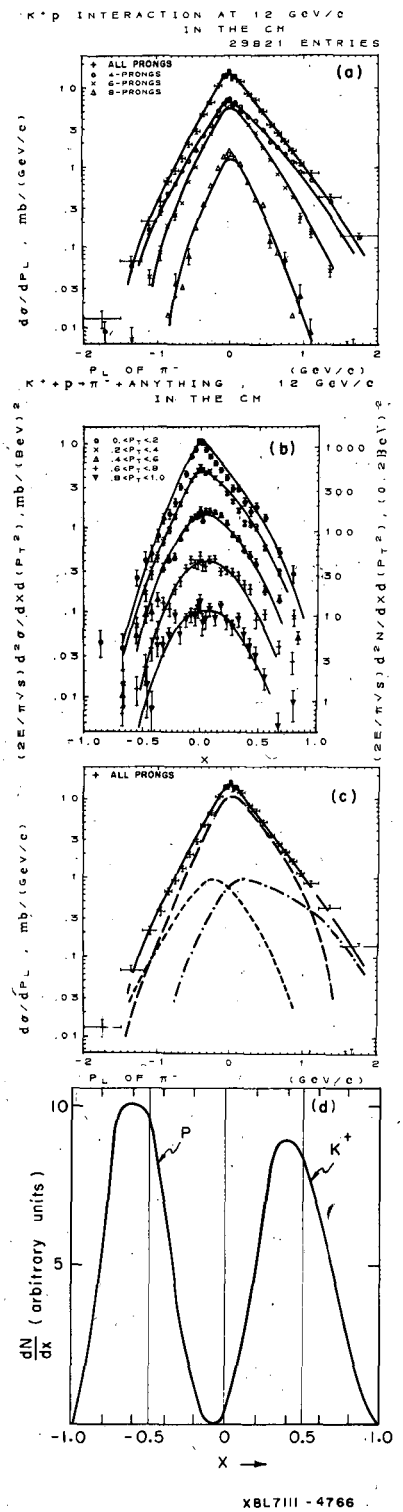
K⁺p INTERACTION AT 12 GeV/c
IN THE CM
29821 ENTRIES
(a)
+ ALL PRONGS
4-PRONGS
6-PRONGS
8-PRONGS
dσ/dP_L , mb/(GeV/c)
P_L OF π⁻ (GeV/c)
K⁺+p→π⁻+ANYTHING , 12 GeV/c
IN THE CM
(b)
0.<P_T<.2
.2<P_T<.4
.4<P_T<.6
.6<P_T<.8
.8<P_T<1.0
(2E/π√s) d²σ/dxd(P_T²), mb/(BeV)²
(2E/π√s) d²N/dxd(P_T²), (0.2BeV)⁻²
x
(c)
+ ALL PRONGS
(d)
P
K⁺
dN/dx (arbitrary units)
x →
XBL7111-4766

Fig. 2 (a-d)

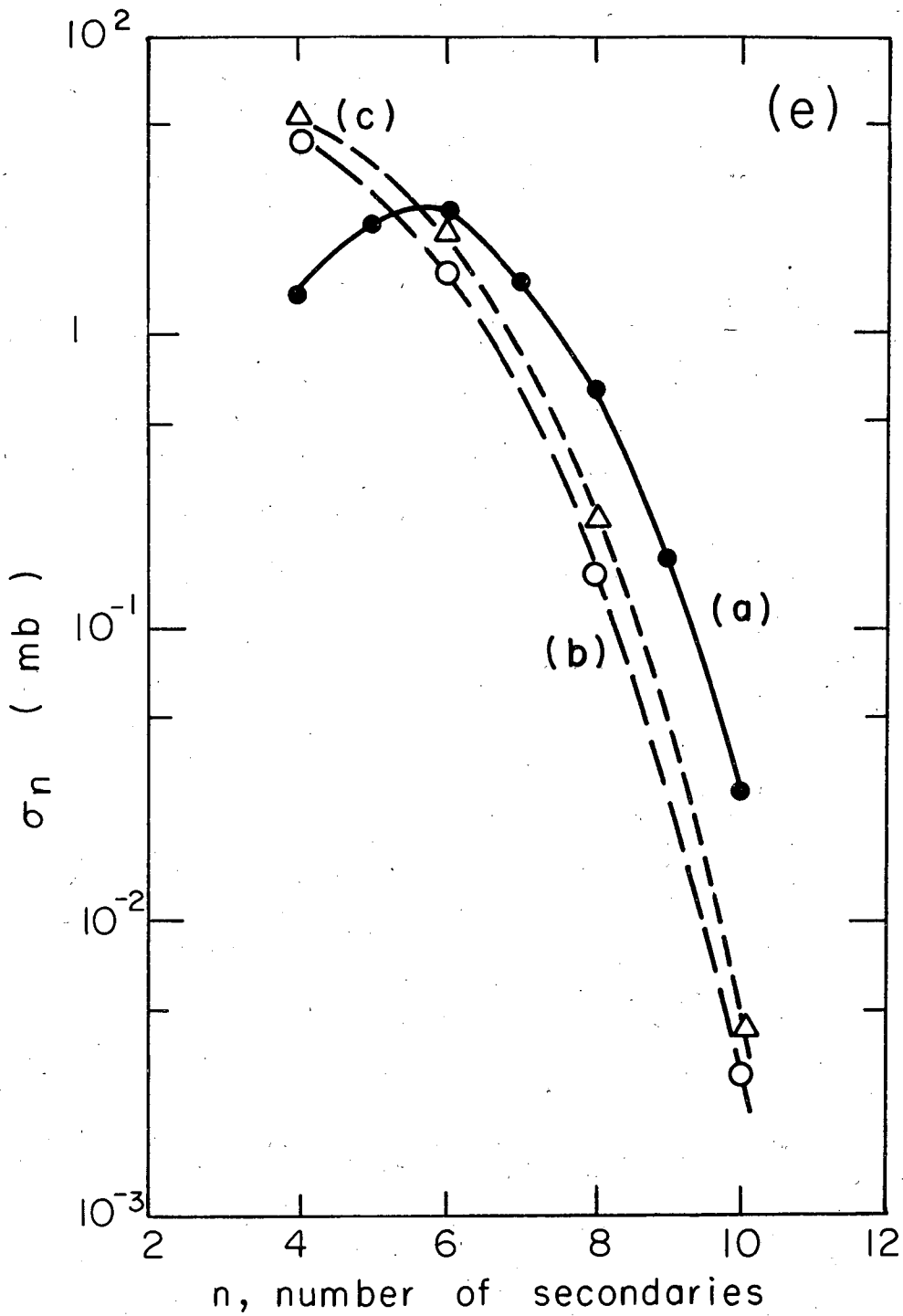

XBL7111-4767

Fig. 2 (e)

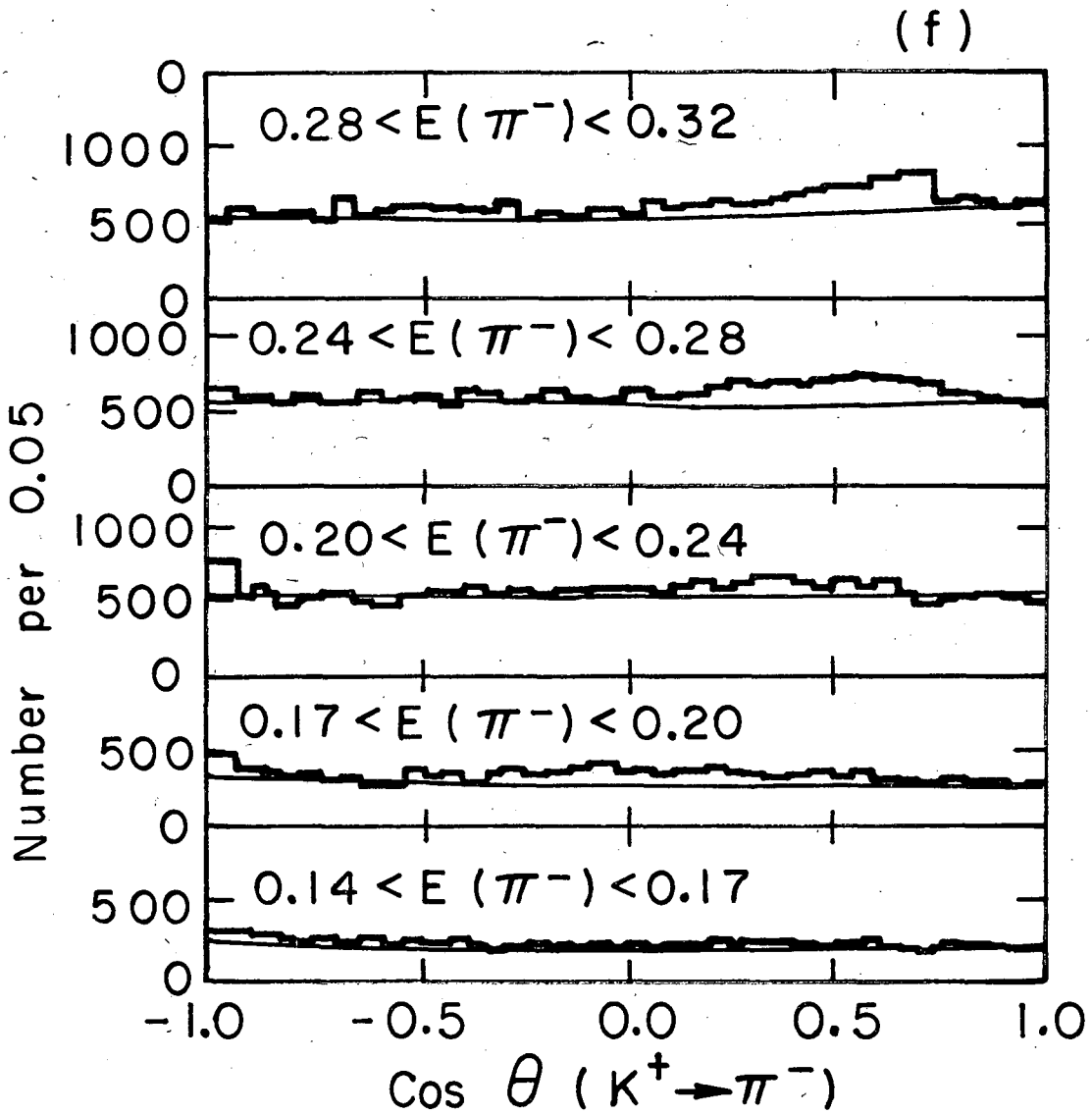

XBL7111-4765

Fig. 2 (f)

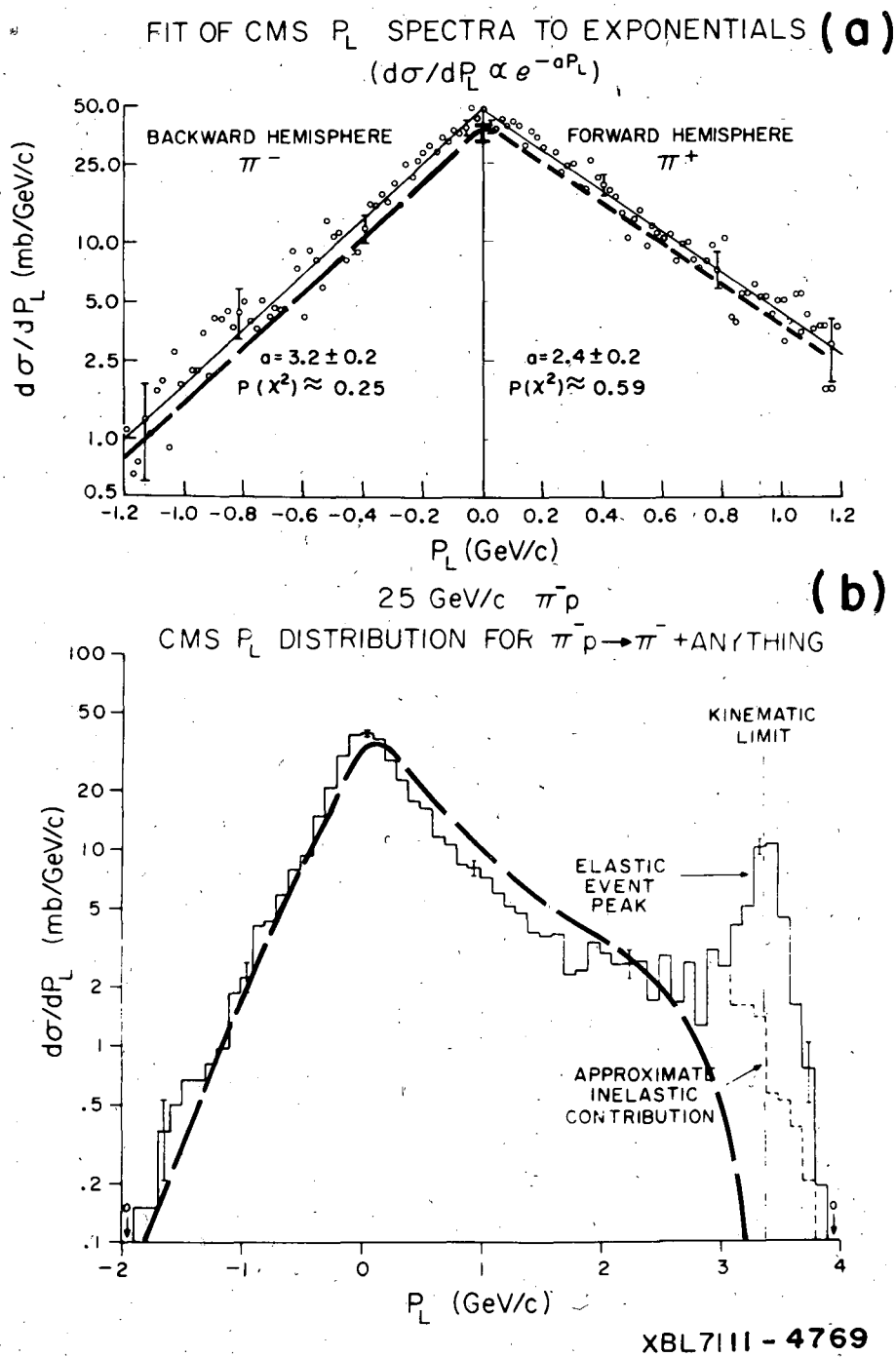
FIT OF CMS P_L SPECTRA TO EXPONENTIALS
(a)
$(d\sigma/dP_L \propto e^{-aP_L})$
BACKWARD HEMISPHERE
π^-
FORWARD HEMISPHERE
π^+
$a = 3.2 \pm 0.2$
$P(\chi^2) \approx 0.25$
$a = 2.4 \pm 0.2$
$P(\chi^2) \approx 0.59$
$d\sigma/dP_L$ (mb/GeV/c)
P_L (GeV/c)
25 GeV/c $\pi^- p$
(b)
CMS P_L DISTRIBUTION FOR $\pi^- p \rightarrow \pi^-$ +ANYTHING
KINEMATIC LIMIT
ELASTIC EVENT PEAK
APPROXIMATE INELASTIC CONTRIBUTION
$d\sigma/dP_L$ (mb/GeV/c)
P_L (GeV/c)
XBL7111-4769

Fig. 3

LEGAL NOTICE

This report was prepared as an account of work sponsored by the United States Government. Neither the United States nor the United States Atomic Energy Commission, nor any of their employees, nor any of their contractors, subcontractors, or their employees, makes any warranty, express or implied, or assumes any legal liability or responsibility for the accuracy, completeness or usefulness of any information, apparatus, product or process disclosed, or represents that its use would not infringe privately owned rights.

TECHNICAL INFORMATION DIVISION
LAWRENCE BERKELEY LABORATORY
UNIVERSITY OF CALIFORNIA
BERKELEY, CALIFORNIA 94720